13. Willemsen ATM, van Waarde A, Paans AMJ, et al. In vivo protein synthesis rate determination in primary or recurrent brain tumors using L-[1-^{11}C]-tyrosine and PET. *J Nucl Med* 1995;36:411–419.
14. Pruim J, Willemsen A, Molenaar WM, et al. Brain tumors: L[1-^{11}C]tyrosine PET for visualization and quantification of protein synthesis rate. *Neuroradiology* 1995;197: 221–226.
15. Gerdes J, Lemke H, Baisch H, Wacker HH, Schwab U, Stein H. Cell cycle analysis of a cell proliferation-associated human nuclear antigen defined by the monoclonal antibody Ki-67. *J Immunol* 1984;133:1710–1715.
16. Zuber P, Hamou MF, de Tribolet N. Identification of proliferating cells in human gliomas using the monoclonal antibody Ki-67. *Neurosurgery* 1988;22:364–368.
17. Raghavan R, Steart PV, Weller RO. Cell proliferation patterns in the diagnosis of astrocytomas, anaplastic astrocytomas and glioblastoma multiforme: a Ki-67 study. *Neuropathol Appl Neurobiol* 1990;16:123–133.
18. Giangaspero F, Doglioni C, Rivano MT. Growth fraction in human brain tumors defined by the monoclonal antibody Ki-67. *Acta Neuropathol* 1987;74:179–182.
19. Catoretti G, Becker MHG, Key G, et al. Monoclonal antibodies against recombinant parts of the Ki-67 antigen (MIB 1 and MIB 3) detect proliferating cells in microwave-processed formalin-fixed paraffin sections. *J Pathol* 1992;168:357–363.
20. Karamitopoulou E, Perentes E, Diamantis I, Maraziotis T. Ki-67 immunoreactivity in human central nervous system tumors: a study with MIB 1 monoclonal antibody on archival material. *Acta Neuropathol* 1994;87:47–54.
21. Bloom SE, Goodpasture C. An improved technique for selective silver staining of nucleolar organizer regions in human chromosomes. *Hum Genet* 1976;34:199–206.
22. Lindler LE. Improvements in the silver-staining technique for nucleolar organizer regions (AgNOR). *J Histochem Cytochem* 1993;41:439–445.
23. Shi SR, Key ME, Kalra KL. Antigen retrieval in formalin-fixed, paraffin-embedded tissues: an enhancement method for immunohistochemical staining based on microwave oven heating of tissue sections. *J Histochem Cytochem* 1991;39:741–748.
24. Emanuels A, Hollema H, Koudstaal J. Autoclave heating: an alternative method for microwaving? *Eur J Morphol* 1994;32:337–340.
25. Howell WM, Black DA. Controlled silverstaining of nucleolus organizer regions with a protective colloidal developer: a 1-step method. *Experientia* 1980;36:1014–1015.
26. Emmers R. The AgNOR staining: a quantitative and qualitative study [in Dutch]. *Histotechniek* 1990;9:109–115.
27. Kleihues P, Burger PC, Scheithauer BW. The new WHO classification of brain tumors. *Brain Pathol* 1993;3:255–268.
28. Kleihues P, Burger PC, Scheithauer BW. *Histological typing of tumors of the central nervous system*. Berlin; Springer Verlag: 1993.
29. Leek RD, Alison MR, Sarraf CE. Variations in the occurrence of silver-staining nucleolar organizer regions (AgNORs) in non-proliferating and proliferating tissues. *J Pathol* 1991;165:43–51.
30. Trerè D, Farabegoli F, Cancellieri A, Ceccarelli C, Eusebi V, Derenzini M. AgNOR area in interphase nuclei of human tumors correlates with the proliferative activity evaluated by bromodeoxyuridine labeling and Ki-67 immunostaining. *J Pathol* 1991;165:53–59.
31. Derenzini M, Pession A, Trerè D. Quantity of nucleolar silver-stained proteins is related to proliferating activity in cancer cells. *Lab Invest* 1990;63:137–140.
32. Korkolopoulou P, Christodoulou P, Papanikolaou A, Thomas-Tsagli E. Proliferating cell nuclear antigen and nucleolar organizer regions in CNS tumors: correlation with histological type and tumor grade. A comparative study of 82 cases on paraffin sections. *Am J Surg Pathol* 1993;17:912–919.
33. Louis DN, Meehan SM, Ferrante RJ, Hedley-Whyte ET. Use of the silver nucleolar organizer region (AgNOR) technique in the differential diagnosis of central nervous system neoplasia. *J Neuropathol Exp Neurol* 1992;51:150–157.
34. Shiraishi T, Tabuchi K, Mineta T, Momozaki N, Takagi M. Nucleolar organizer regions in various human brain tumors. *J Neurosurg* 1991;74:979–984.
35. Daemen BJG, Zwertbroek R, Elsinga PH, Paans AMJ, Doorenbos H, Vaalburg W. PET studies with L[1-^{11}C]tyrosine, L[methyl-^{11}C]methionine and ^{18}FDG in prolactinomas in relation to bromocryptine treatment. *Eur J Nucl Med* 1991;18:453–460.
36. Bustany P, Chatel M, Derlon JM, et al. Brain tumor protein synthesis and histological grades: a study by PET with ^{11}C-L-methionine. *J Neurooncol* 1986;3:397–404.
37. Sato K, Kameyama M, Ishiwata K, Hatazawa J, Katekura R, Yoshimoto T. Dynamic study of methionine uptake in glioma using positron emission tomography. *Eur J Nucl Med* 1992;19:426–430.
38. Daemen BJG, Elsinga PH, Ishiwata K, Paans AMJ, Vaalburg W. A comparative study using different ^{11}C-labeled amino acids in Walker 256 carcinosarcoma-bearing rats. *Nucl Med Biol* 1990;18:197–204.
39. Ishiwata K, Kubota K, Murakami M, et al. Re-evaluation of amino acid PET studies: can the protein synthesis rate in brain and tumor tissues be measured in vivo? *J Nucl Med* 1993;34:1936–1943.
40. Delahunt B, Bethwaite PB, Nacey JN, Ribas JL. Proliferating cell nuclear antigen (PCNA) expression as a prognostic indicator for renal cell carcinoma: comparison with tumor grade, mitotic index and silver-staining nucleolar organizer region members. *J Pathol* 1993;170:471–477.
41. Van Langevelde A, van der Molen HD, de Korver-Journee JG, Paans AM, Pauwels EK, Vaalburg W. Potential radiopharmaceuticals for the detection of ocular melanoma. Part III. A study with ^{14}C and ^{11}C-labeled tyrosine and dihydroxyphenylalanine. *Eur J Nucl Med* 1988;14:382–387.
42. Onda K, Davis RL, Wilson CB, Hoshino T. Regional differences in bromodeoxyuridine uptake, expression of Ki-67 protein and nucleolar organizer region counts in glioblastoma multiforme. *Acta Neuropathol* 1994;87:586–593.
43. Josza L, Kannus P, Jarvinen M, Isola J, Kvist M, Lehto M. Atrophy and regeneration of rat calf muscles cause reversible changes in the number of nucleolar organizer regions. *Lab Invest* 1993;69:231–237.
44. Ruschoff J, Elsasser HP, Adler G. Correlation of nucleolar organizer regions with secretory and regenerative process in experimental cerulein-induced pancreatitis in the rat. *Pancreas* 1995;11:154–159.
45. Takeda N, Diksic M, Yamamoto YL. The sequential changes in DNA synthesis, glucose utilization, protein synthesis and peripheral benzodiazepine receptor density in C6 brain tumors after chemotherapy to predict the response of tumors to chemotherapy. *Cancer* 1996;77:1167–1179.

Prediction of Myelotoxicity Using Radiation Doses to Marrow from Body, Blood and Marrow Sources

Sang-Moo Lim, Gerald L. DeNardo, Diane A. DeNardo, Sui Shen, Aina Yuan, Robert T. O'Donnell and Sally J. DeNardo
University of California Davis Medical Center, Sacramento, California; and Veteran's administration, Northern California Health Care System, California

Bone marrow is generally the dose-limiting organ in radioimmunotherapy (RIT). Although radiation doses to marrow estimated from tracer doses have been shown to be comparable to those from therapy doses of radionuclide, the correlation of marrow radiation dose and myelotoxicity has not been well documented. The purpose of this study was to evaluate the relationship between radiation dose to marrow and subsequent changes in peripheral blood cell counts. **Methods:** Radiation doses to marrow from three sources, body, blood and marrow targeting, were compared with changes in blood counts after the first therapy dose of ^{131}I-Lym-1 in 16 patients. Doses of ^{131}I-Lym-1 ranged from 1.1–8.2 GBq (29–222 mCi). Cumulated radioactivity in the body and marrow were obtained using sequential, quantitative images of the body and lumbar vertebrae, respectively, and that in blood using activity in blood samples. The individual and sum of radiation doses from penetrating radiations in the body, and nonpenetrating radiations in the blood and marrow, were compared with blood counts. **Results:** In this group of patients, median radiation doses were 15.1, 15.4 and 42.1 cGy from body, blood and marrow targeting, respectively. Linear regression of radiation doses from body and blood versus fractional decreases in blood counts produced correlation coefficients of 0.38, 0.06, 0.22 and less than 0.01 for platelets, granulocytes, white blood cells (WBCs) and hematocrit, respectively. Linear regression of targeted marrow radiation doses versus fractional decreases in blood counts produced correlation coefficients 0.61, 0.31, 0.54 and 0.20 for platelets, granulocytes, WBCs and hematocrit. The closest association was found between radiation dose to marrow from marrow targeting and change in platelet count ($r = 0.61$). **Conclusion:** In patients, such as those with non-Hodgkin's lymphoma (NHL), likely to have marrow targeting, prediction of myelotoxicity by conventional body and blood contributions to marrow is substantially improved by the use of radiation dose to marrow estimated from images.

Key Words: dosimetry; myelotoxicity; radioimmunotherapy; iodine-131-Lym-1

J Nucl Med 1997; 38:1374–1378

Received Sep. 23, 1996; revision accepted Jan. 20, 1997.

For correspondence or reprints contact: G.L DeNardo, MD, Molecular Cancer Institute, School of Medicine, UC Davis, 1508 Alhambra Blvd. #214, Sacramento, CA 95816.

Methods for determining the radiation dose delivered to human bone marrow from radiopharmaceuticals have traditionally addressed contributions from radionuclidic sources in the body, blood or both (*1–3*). As a result of studies sponsored by the American Association of Physicists in Medicine, Siegel et al. (*3*) proposed a standardization of the blood radioactivity method. DeNardo et al. (*4*) and Macey et al. (*5*) proposed modifications to account for potential redundancies in considering nonpenetrating and penetrating emissions when addressing both body and blood contributions. Sgouros et al. (*6*) proposed modifications to account for the effect of hematocrit on the relationship of marrow activity to that of blood. Recently, there have been efforts to correlate the radiation doses to marrow estimated by these methods with subsequent evidence for myelotoxicity (*6,7*). Although some positive correlation was reported, it was less than definitive, presumably because of confounding factors, such as prior chemotherapy and effects of the malignancy itself, that contribute to myelotoxicity. One effect that is evaluable is the radiation dose to the marrow from radionuclide targeted to malignant cells in the marrow and skeleton (*8*). Several groups have described imaging methods for measuring the marrow radiation from targeted radionuclide (*5,9–11*), however, the value of these imaging methods for prediction of myelotoxicity is unclear (*3,9,12*). The current study evaluated the relationship of radiation doses from marrow targeting to subsequent evidence for myelotoxicity in patients with NHL; these data were considered relative to conventional dosimetric data and bone marrow biopsy.

MATERIALS AND METHODS

Patients

A subset of 20 patients (20/54), who had longer intervals since their last chemotherapy and greater likelihood of marrow NHL, treated with ^{131}I-Lym-1 were selected for this study if they met the following criteria:

1. No other myelotoxic therapy for at least 4 wk before or after RIT in order to minimize confounding factors;
2. No history of prior irradiation to the lumbar spine (lumbar region of interest (ROI) was used for study analysis); and
3. Bone marrow biopsy.

Twenty patients met the above criteria, but four of these patients were excluded: two had bulky paravertebral masses of sufficient size to interfere with estimation of background radioactivity, and two had increases in blood counts after RIT that probably reflected recovery from chemotherapy. Analyses were performed on the remaining 16 patients, six of whom were positive for marrow NHL by biopsy.

Radiopharmaceuticals

Lym-1 is an IgG2a mouse monoclonal antibody that targets B-cell lymphocytic malignancies (*13*). Lym-1 was produced in our laboratory or obtained from Damon Biotech, Inc. (Needham Heights, MA) or Techniclone, Inc. (Tustin, CA). Lym-1 was radioiodinated with high specific activity ^{131}I by the chloramine-T method. At least 90% of the ^{131}I was bound to Lym-1, and immunoreactivity was at least 87% of the reference standard. A range of injected doses (1.1–8.2 GBq; 29–222 mCi) was administered under a physician-sponsored IND.

Marrow Dosimetry

The radiation dose to marrow was determined for three contributing sources: body, blood and targeting of marrow malignancy. The marrow dose from the body was determined for penetrating radiations from the body assuming a uniform distribution of radionuclide in the body (*4,14*). The dose to marrow from blood

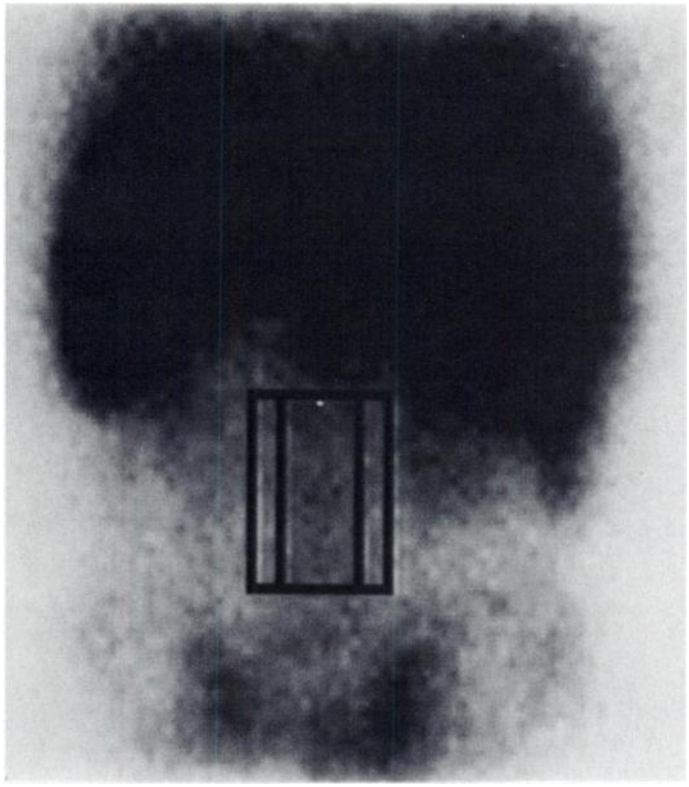

FIGURE 1. Standard marrow and background ROIs superimposed on posterior abdominal image. Based on CT analysis, a standard marrow ROI (L2, L3, L4) width of 5 cm was used. Background ROI width was 1 cm on each side of the marrow ROI and was the same height as the marrow ROI. Height of the ROIs varied based on CT measurements. Liver, spleen, kidneys and pelvis (sacroiliac joints) serve as landmarks. Targeted abdominal mass (above ROI) was excluded from the ROI.

was determined for nonpenetrating radiations alone by methods described by DeNardo et al. (*4*). The specific activity of blood in marrow was assumed to be 0.25 (*6*), and uniform distribution and complete absorption of nonpenetrating radiations in marrow were assumed.

Cumulative activity in marrow and the MIRD S factor for nonpenetrating radiations were used to determine radiation dose to marrow from marrow targeting (*14*). Two assumptions were used:

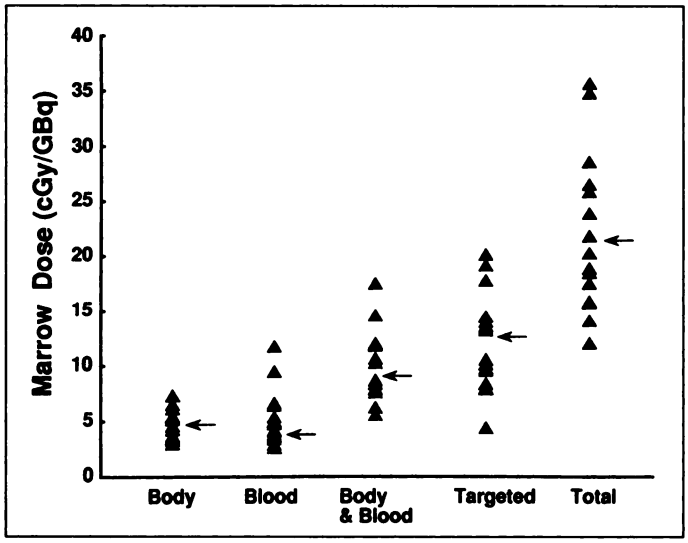

FIGURE 2. Median (←) and ranges of radiation doses to marrow from body, blood and marrow targeting. The median targeted marrow radiation dose was more than twice that from the body or blood to marrow in this group of patients with NHL.

TABLE 1
Comparison of Radiation Doses to Marrow with Decreases in Blood Counts

Sources of radiation dose to marrow	Correlation coefficients for fractional decrease in blood counts			
	Platelets	Granulocytes	White blood cells	Hematocrit
Body	0.34	0.18	0.31	0.13
Blood	0.38	0.06	0.13	0.12
Body and Blood	0.38	0.06	0.22	<0.01
Targeted marrow	0.61	0.31	0.54	0.20
Total body, blood and targeted marrow	0.54	0.49	0.47	0.11

1. Marrow dose can be extrapolated from radionuclide in three lumbar vertebrae; and
2. The marrow in three lumbar vertebrae (L2, L3, L4) is equal to 6.7% of total active marrow (*15*).

Comparisons of Marrow Radiation with Decreases in Blood Counts

To determine whether radiation doses to marrow could be used to predict myelotoxicity, linear regressions were performed on data for radiation doses to marrow versus fractional decreases in counts for platelets, WBCs, granulocytes and hematocrit. The radiation doses to marrow included individual and sums of body, blood and marrow targeting. Correlation coefficients were then compared for all regressions to select the best predictors of myelotoxicity. The post-therapy nadir for each blood count parameter was compared with the baseline counts:

$$\text{Fractional decrease, blood count} = \frac{\text{initial} - \text{nadir}}{\text{initial}}. \qquad \text{Eq. 1}$$

Quantitative Marrow Image Processing and Reproducibility

The imaging study obtained after the first treatment dose in each patient was reviewed by one of the authors without knowledge of other data. Planar image quantitation was performed on sequential, posterior images of the abdomen to measure the amount of radionuclide in three lumbar vertebrae (*9*). Images were acquired on either a Siemens ZLC 7500 or Bodyscan camera interfaced to MicroDelta computers immediately, 4–6 hr and daily for 7 days after injection. To determine size and location of the marrow ROI, the height of three lumbar vertebrae (L2,L3,L4) and three vertebral spaces was measured on x-ray CT images of 20 patients. A fixed relationship was found between patient height and the height of three lumbar vertebrae; this relationship was used to determine the height of the marrow ROI when CT images were not available for individual patients. Mean vertebral width (including cortical bone) was found to be 5.2 ± 0.2 cm measured from 20 patient CT scans. Therefore, a standard marrow ROI width of 5 cm and a background ROI width of 1 cm on each side with the same height as the marrow ROI was used (Fig. 1). The effect of narrower background ROIs (0.6 and 0.3 cm) was examined by comparing cumulated activities obtained with these narrower background ROIs to those obtained by the standard marrow ROI. The average variation in cumulated activity was only 9%. When vertebrae were well visualized on the planar images, the top of the ROI was aligned with the top of the second lumbar vertebra. When the vertebrae were less well visualized, the top of the second lumbar vertebra was noted in relation to other organs on the CT images and accordingly aligned on the planar image relative to other organs. Peak uptake of ^{131}I-Lym-1 in marrow occurred by 6 hr in 14 of the patients under study.

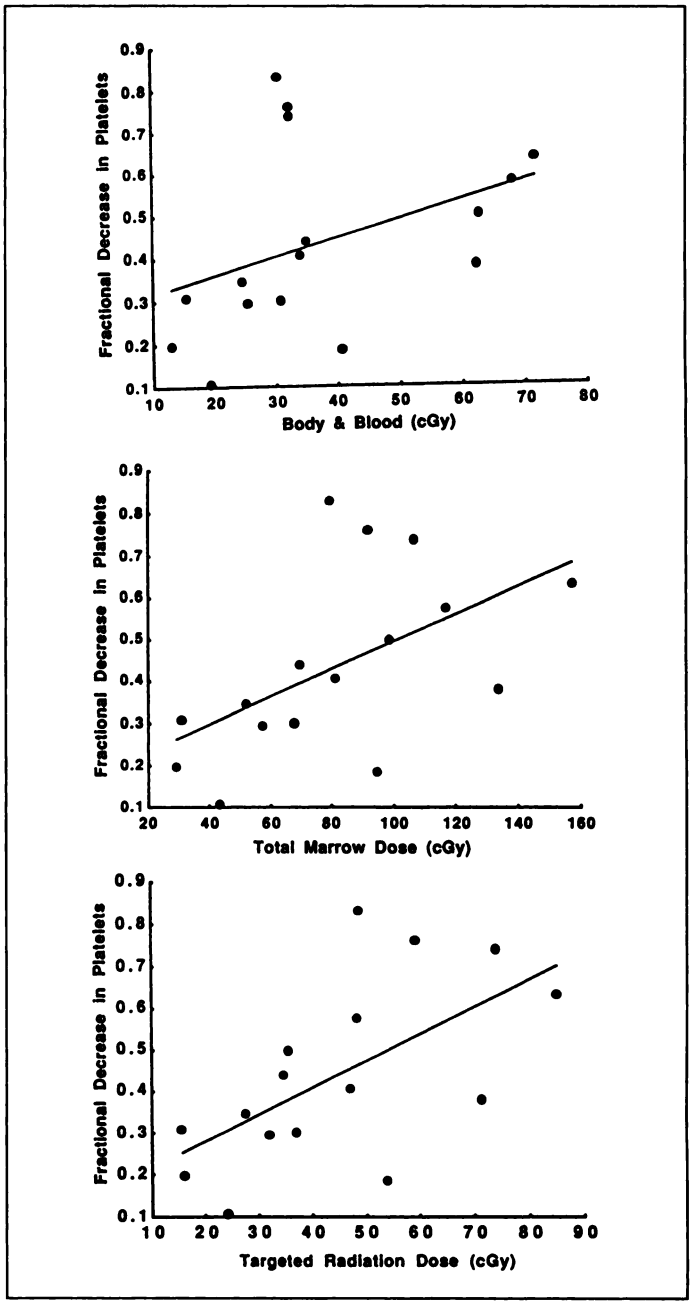

FIGURE 3. Correlation between radiation dose and nadir fractional platelet decrease. Linear correlation between radiation dose to marrow from body and blood (upper) was weak (r = 0.38), was improved somewhat by the addition of the targeted marrow dose (middle) (r = 0.55) and was best for targeted marrow dose alone (bottom) (r = 0.61).

The reproducibility of marrow image processing using the lumbar ROI method was evaluated. A single operator processed each set of images three times at intervals of ≥7 days. Intraoperator reproducibility was determined by the coefficient of variation. Intraoperator reproducibility of quantitative marrow image processing was ≤10% for radiation dose to marrow from marrow targeting.

RESULTS

Marrow Dosimetry

The targeted marrow dose contributed more to the marrow dose than did the body or blood in these patients (Fig. 2). The

median and range of radiation doses to marrow from body, blood and marrow targeting were 4.9 (3.0–7.3), 4.1 (2.7–11.9) and 11.9 (4.3–20.3) cGy/GBq, respectively. The median radiation dose to marrow from all three sources was 21.1 (11.9–35.4) cGy/GBq.

Comparisons of Marrow Radiation with Decreases in Blood Counts

The correlation coefficients for fractional decrease in blood counts versus body and blood radiation doses to marrow were low in these patients ($r < 0.4$, Table 1, Fig. 3). In contrast, the correlation coefficient for targeted marrow dose versus fractional decrease in platelets was 0.61. Addition of the body and blood contributions to the targeted radiation dose to marrow failed to improve the correlation coefficients; however, the granulocyte comparison increased from 0.31 to 0.49 (Table 1, Fig. 3). Correlation coefficients were highest for platelets and lowest for hematocrit for all marrow radiation versus blood count comparisons.

The median fractional decrease in blood counts after therapy was greatest for platelets (0.39, 0.11–0.83), followed by granulocytes (0.30, 0.10–0.80). The median fractional decrease was less for WBCs (0.23, 0.06–0.60) and hematocrit (0.09, 0.01–0.23).

DISCUSSION

The radiation dose to bone marrow and blood counts after RIT are measurable and are potential indicators of myelotoxicity. However, the ability to predict myelotoxicity after RIT from radiation dose estimates has previously not been well documented. There was little correlation between any of the methods for assessing radiation to the bone marrow described herein and a decrease in hematocrit after ^{131}I-Lym-1 therapy. As with conventional external beam radiotherapy, erythrocyte progenitors are less sensitive to exponentially decreasing low-dose rate irradiation than other marrow elements (*16*). Furthermore, because of erythrocyte longevity, decreased erythropoiesis is less likely than thrombocytopenia or leukopenia to be prominent early. The conventional sources for estimating marrow radiation, i.e., body and blood, alone or in aggregate, did not correlate well with therapy-induced thrombocytopenia or leukopenia, although the former correlation was the best. Radiation dose estimated from images of the lumbar vertebral marrow (targeted marrow radiation) correlated rather well with therapy-induced thrombocytopenia and leukopenia and was better than the correlations for body, blood or body and blood for all blood cell parameters studied. As expected, the correlation of radiation dose with thrombocytopenia was best. Addition of the contributions from body and blood to that of targeted marrow radiation did not improve the correlations beyond that of targeted marrow radiation alone except for an improved correlation with granulocytopenia. These observations are consistent with those of Juweid (*12*) for patients with NHL. Incomplete correlation of targeted marrow radiation dose with therapy-induced decreases in peripheral blood counts, underscores the limitations of evaluating the marrow dosimetry method in heavily pretreated patients with hematologic malignancies (*8,17*).

In this patient population, several factors underlie the superior performance of targeted marrow radiation dose measurement (*8*). First, bone marrow involvement in patients with NHL is common (*18*), and body and blood methods for estimating marrow radiation fail to account for marrow targeting. In the patients in our study, six had positive bone marrow biopsies, and their radiation doses from targeted marrow exceeded 8 cGy/GBq in each instance. Indeed, other patients with elevated marrow doses from targeting probably had marrow malignancy, which, as demonstrated by Tardivon et al. (*19*), has shown that MRI reveals lymphomatous marrow involvement even when marrow biopsies are negative. The absolute amounts of radiation from body and/or blood to marrow were also insufficient to explain the myelotoxicity in these patients even if heavy pretreatment was considered. In this select group of patients, radiation doses from targeted marrow were several times greater than those from body or blood, although still less than expected, when given the median fractional decrease in platelet and granulocyte counts were 39% and 30%, respectively. Others have reported larger radiation doses for comparable manifestations of myelotoxicity from radioimmunotherapy (*20,21*).

The radiation dose estimates for targeted marrow radiation were reproducible when determined by a single, experienced observer. This reflects the fact that minor variations in vertebral or background ROIs produced insignificant alterations in the final radiation dose estimate despite sometimes larger alterations in a single observation of percent injected dose in the sequence of observations used to obtain cumulated activity. Although the results in this study reflect the use of an ROI that identified three contiguous lumbar vertebrae and an adjacent background ROI, this is not a rigid requirement for the method. All lumbar vertebrae are essentially the same size. Therefore any three could be identified by the ROI in order to avoid a focally involved vertebrae. Furthermore, the size of the background ROI can be altered somewhat, as long as it is adjacent to the vertebrae and is not in an area of paravertebral malignancy. Marrow ROI was not altered in the two excluded patients in order to maintain a standardized methodology for this study. It is important to appreciate that the numerical value for targeted marrow radiation dose can only be used to project likelihoods of myelotoxicity. Several investigators have emphasized the complexity of skeletal marrow at both a macroscopic and microscopic level (*3,6,22*). Kassis emphasized that the conventional MIRD technique, whether applied to body and blood or to targeted marrow radiation, determines average radiation doses, and "nonuniform radionuclide distribution causes dose nonuniformity regardless of the range of particles (*22*)."

CONCLUSION

In this subset of patients with NHL, prediction of myelotoxicity by conventional body and blood radiation doses to marrow after RIT was improved by the addition of image-based estimates of the radiation dose to marrow. RIT image-based estimates of radiation dose to marrow can be used globally to project likelihoods of myelotoxicity. Improved methods are needed to more accurately predict myelotoxicity.

ACKNOWLEDGMENTS

This study was supported by National Cancer Institute grant NCI CA47829 and Department of Energy grant FG03–84ER60233. S-M.L. (Korea Cancer Hospital, Seoul, Korea) was supported by the International Atomic Energy Agency Fellowship Program #ROK-95004P.

REFERENCES

1. DeNardo DA, DeNardo GL, Yuan A, et al. Prediction of radiation doses from therapy using tracer studies with iodine-131-labeled antibodies. *J Nucl Med* 1996;37:1970–1975.
2. Robertson JS, Godwin JT. Calculation of radioactive iodine BETA radiation dose to the bone marrow. *Br J Radiol* 1954;27:241–242.
3. Siegel JA, Wessels BW, Watson EE, et al. Bone marrow dosimetry and toxicity for radioimmunotherapy. *Antibody Immunoconj Radiopharm* 1990;3:213–233.
4. DeNardo GL, Mahe MA, DeNardo SJ, et al. Body and blood clearance and marrow radiation dose of ^{131}I-Lym-1 in patients with B-cell malignancies. *Nucl Med Commun* 1993;14:587–595.

5. DeNardo SJ, Macey DJ, DeNardo GL. A direct approach for determining marrow radiation from MoAb therapy. In: Denardo GL, ed. *Biology of radionuclide therapy*. Washington, D.C.: American College of Nuclear Physicians, 1989:110–124.
6. Sgouros G. Bone marrow dosimetry for radioimmunotherapy: theoretical considerations. *J Nucl Med* 1993;34:689–694.
7. Siegel JA, Lee RE, Pawlyk DA. Sacral scintigraphy for bone marrow dosimetry in radioimmunotherapy. *Nucl Med Biol* 1989;16:553–559.
8. DeNardo GL, DeNardo SJ, Macey DJ, Shen S, Kroger LA. Overview of radiation myelotoxicity secondary to radioimmunotherapy using ^{131}I-Lym-1 as a model. *Cancer* 1994;73:1038–1048.
9. Macey DJ, DeNardo SJ, DeNardo GL, DeNardo DA, Shen S. Estimation of radiation absorbed doses to the red marrow in radioimmunotherapy. *Clin Nucl Med* 1995;20: 117–125.
10. Siegel JA, Lee RE, Pawlyk DA, Horowitz JA, Sharkey RM, Goldenberg DM. Sacral scintigraphy for bone marrow dosimetry in radioimmunotherapy. *Int J Rad Appl Instrum [B]* 1989;16:553–559.
11. Buijs WC, Bassuger LF, Claessens RA, et al. Dosimetric evaluation of immunoscintigraphy using indium-111-labeled monoclonal antibody fragments in patients with ovarian cancer [Abstract]. *J Nucl Med* 1992;33(suppl):1113P.
12. Juweid M, Sharkey RM, Siegel JA. Estimates of red marrow dose by sacral scintigraphy in radioimmunotherapy patients having non-Hodgkin's lymphoma and diffuse bone marrow uptake. *Cancer Res* 1995;55(suppl):5827–5831.
13. Epstein AL, Zimmer AM, Spies SM, et al. Radioimmunodetection of human B-cell lymphomas with a radiolabeled tumor-specific monoclonal antibody (Lym-1). In: Cavalli F, Bonadonna G, Rozencweig GM, eds. *Malignant lymphomas and Hodgkin's disease: experimental and therapeutic advances*. Boston, MA: Martinus Nijhjoff, 1985:569–577.
14. Snyder WS, Ford MR, Warner GC. "S" absorbed dose per unit cumulated activity for selected radionuclides and organs. In: *MIRD pamphlet 11*. New York: Society for Nuclear Medicine, 1978.
15. Brodsky, A. *CRC handbook of radiation measurements and protection, section A, volume II: biological and mathematical information*. CRC Press, 1982:148–150.
16. Tubiana M, Frindel E, Croizat H, Parmentier C. Effects of radiations on bone marrow. *Pathol Biol* 1979;27:326–334.
17. Juweid M. Factors affecting myelotoxicity in patients receiving radioimmunotherapy with ^{131}I-labeled anti-CEA monoclonal antibodies. *Cancer* 1997:in press.
18. Morra E, Lazzareno M, Orlandi E, et al. Bone marrow and blood involvement by non-Hodgkin's lymphoma: clinicopathologic features and prognostic significance in relationship to the working formulation. In: Cavalli F, Bonadonna G, Rozencweig M, eds. *Malignant lymphomas and Hodgkin's disease: experimental and therapeutic advances*. Boston: Martinus Nijhoff Publishing; 1985:215–224.
19. Tardivon AA, Munck J-N, Shapeero LG, et al. Can clinical data help to screen patients with lymphoma for MR imaging of bone marrow? *Ann Oncol* 1995;6:795–800.
20. Stein R, Sharkey RM, Goldenberg DM. Hematological effects of radioimmunotherapy in cancer patients. *Br J Haematol* 1992;80:69–76.
21. Breitz HB, Durham JS, Fisher DR, Weiden PL. Radiation dose estimates to normal organs following intra-peritoneal Re-186-labeled monoclonal antibody: methods and results. *Cancer Res* 1995;55(23S):5817–5822.
22. Kassis AL. The MIRD approach: remembering the limitations. *J Nucl Med* 1992;33: 781–782.

Tumor Pretargeting: Role of Avidin/Streptavidin on Monoclonal Antibody Internalization

Patrizia Casalini, Elena Luison, Sylvie Ménard, Maria I. Colnaghi, Giovanni Paganelli and Silvana Canevari
Oncologia Sperimentale E, Istituto Nazionale Tumori, and Medicina Nucleare, Istituto Europeo di Oncologia, Milan, Italy

Radioimmunodetection of tumor can be improved by introducing a two-step system in which radiolabeled streptavidin is administrated after the injection of a biotinylated monoclonal antibody (MAb) (two-step) or radiolabeled biotin is injected after biotinylated MAb and avidin (three-step). The anti-carcinoembryonic antigen (CEA) MAb FO23C5 has been recently exploited in a three-step protocol based on the avidin–biotin system. The anti-folate receptor (FR) MAb MOv18 has proven suitable for radioimmunodetection of ovarian cancer using directly radiolabeled MAb or in a two-step method. In this study, we analyzed the suitability of MOv18 in a three-step protocol in ovarian carcinoma patients and the internalization events after formation of the MOv18–avidin complex. **Methods:** Selected patients with documented metastatic lesions were enrolled in a three-step radioimaging analysis with biotinylated MOv18 and FO23C5, avidin and ^{111}In-labeled biotin. Two-step internalization experiments were conducted in vitro with MOv18 and MOv19 MAbs on the FR-overexpressing IGROV1 cell line and with the anti-CEA MAb FO23C5 on the LS174T cell line. Cells were incubated sequentially with biotinylated MAb and ^{125}I-labeled streptavidin or with ^{125}I-biotinylated MAb and cold streptavidin. **Results:** In the in vivo study, SPECT revealed the majority of metastatic lesions in patients injected with biotinylated MOv18; however, the tumor-to-background ratio was relatively low. In the in vitro study, a consistent internalization was induced by antigen-biotinylated MAb–streptavidin complex formation at the cell surface in both antigenic systems analyzed. However, the extent of internalization was lower in the CEA model. **Conclusion:** The internalization ability of avidin suggests its potential clinical application for delivering toxic agents in a two-step approach (biotinylated MAb + avidin conjugate). The suitability of a given MAb for three-step clinical applications (biotinylated MAb + avidin + biotin) should be previously investigated by using appropriate in vitro experiments.

Received Jul. 10, 1996; revision accepted Feb. 24, 1997.
For correspondence or reprints contact: Maria I. Colnaghi, PhD, Oncologia Sperimentale E, Istituto Nazionale Tumori, Via Venezian, 1, 20133, Milan, Italy.

Key Words: monoclonal antibody; avidin; streptavidin; cellular internalization; tumor pretargeting

J Nucl Med 1997; 38:1378–1381

The avidin/streptavidin–biotin complex has become an extremely useful and versatile detection intermediate in a variety of biological and analytical systems (*1–3*). Its high binding affinity (10^{-15} *M*) ensures binding at extremely low reagent concentrations and binding stability even under extreme conditions (*4*). Recently, the use of this system has been extended to include in vivo procedures such as radioimmunodetection (RID) (*5–8*). Radiolocalization studies have shown that target-to-nontarget radioactivity ratios and radioimaging analyses can be significantly improved by introducing a two-step or three-step system in which radiolabeled avidin or streptavidin is administered after the injection of a biotinylated ligand or radiolabeled biotin is injected after a streptavidin-conjugated antibody or an avidin chase of unbound ligand (*9–12*). The advantages and limitations of the two methods are described elsewhere (*13,14*). The avidin–biotin system, applied to RID, allows the use of short-half-life radionuclides and has been shown to enhance the applicability and effectiveness of radio-immuno-guided surgery (*10*). However, in this system, the three-step approach is feasible only when the ligand–avidin complex is still present on the membrane at the time that radiolabeled biotin is administered.

The major area of clinical application of the avidin–biotin complex is the detection of tumor markers bound by monoclonal antibodies (MAbs). Several markers of human carcinomas have been identified so far, and some of them have been exploited in RID and radioimmunotherapy, based on the tumor-restricted and homogeneous overexpression of these markers (*15,16*). The folate receptor (FR), which is recognized by MAbs